Supplementary Material for "Wiedemann-Franz law and abrupt change in conductivity across the pseudogap critical point of a cuprate superconductor"

B. Michon,[1,2] A. Ataei,[1] P. Bourgeois-Hope,[1] C. Collignon,[1] S. Y. Li,[1] S. Badoux,[1] A. Gourgout,[1] F. Laliberté,[1] J.-S. Zhou,[3] Nicolas Doiron-Leyraud,[1] and Louis Taillefer[1,4]

[1] *Institut Quantique, Département de physique & RQMP, Université de Sherbrooke, Sherbrooke, Québec, Canada J1K 2R1*

[2] *Univ. Grenoble Alpes, Institut Néel, F-38042 Grenoble, France*

[3] *Texas Materials Institute, University of Texas, Austin, USA*

[4] *Canadian Institute for Advanced Research, Toronto, Ontario, Canada M5G 1Z8*

(Dated: July 31, 2018)

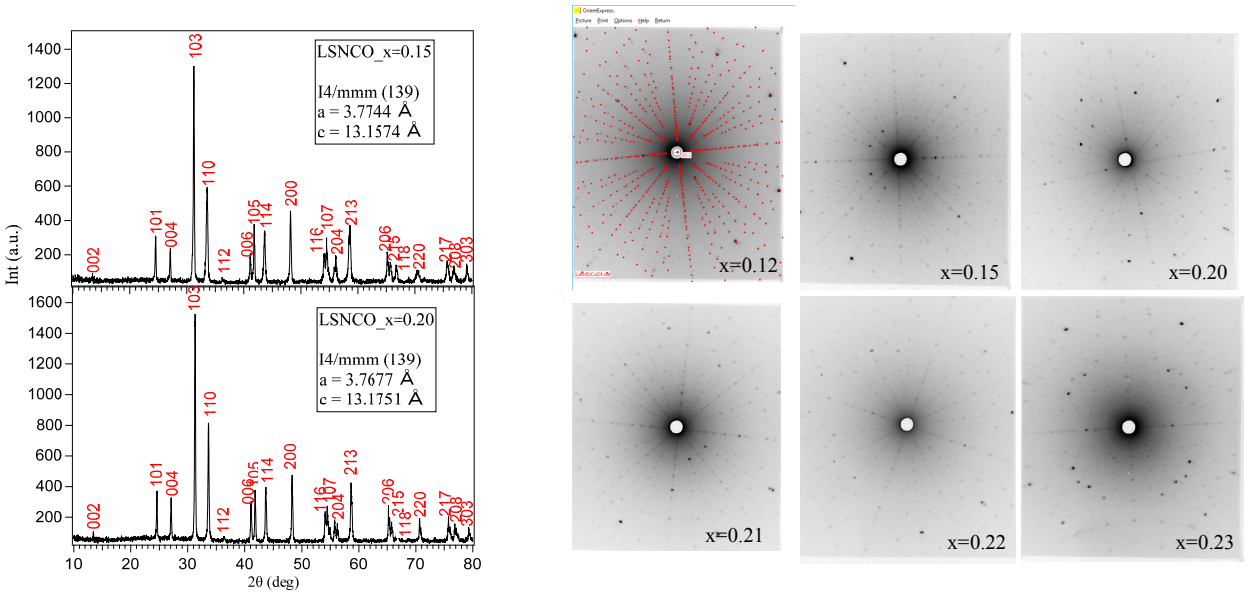

FIG. S1. Left: Typical x-ray diffraction (XRD) patterns of the powder Nd-LSCO samples pulverized from the piece of crystal adjacent to the bar used for the thermal conductivity and other transport property measurements. The diffraction peak width is narrow and no peak from impurity phases can be discerned from the patterns. The lattice parameters from the least-square refinement on XRD pattern are shown in the box inside. Right: Patterns of Laue back reflection taken on the same Nd-LSCO crystals. The oriented pattern along the 0,0,-1 direction is overlaid on the x=0.12 crystal. All patterns were taken on crystals oriented with the surface normal to the x-ray beam, except for the x=0.23 crystal which has the surface normal to the 1,0,0 direction.

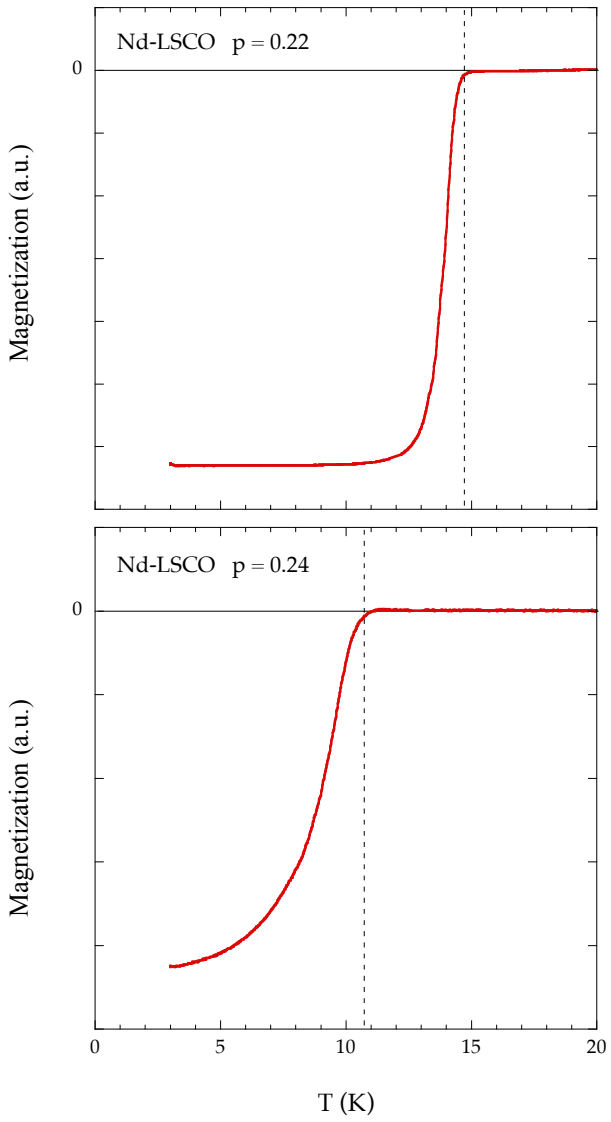

FIG. S2. Vibrating sample magnetometer (VSM) data as $H \to 0$ for the two Nd-LSCO samples (with $p = 0.22$ and $p = 0.24$) for which we compare resistivity data (Fig. 1(b)) and thermal conductivity data (Fig. 2). As is the case for all samples, the superconducting transition is smooth, showing no indication of an impurity phase with a different T_c. The T_c value of the $p = 0.24$ sample is distinctly lower than the T_c value of the $p = 0.22$ sample, confirming that the former has a higher doping.

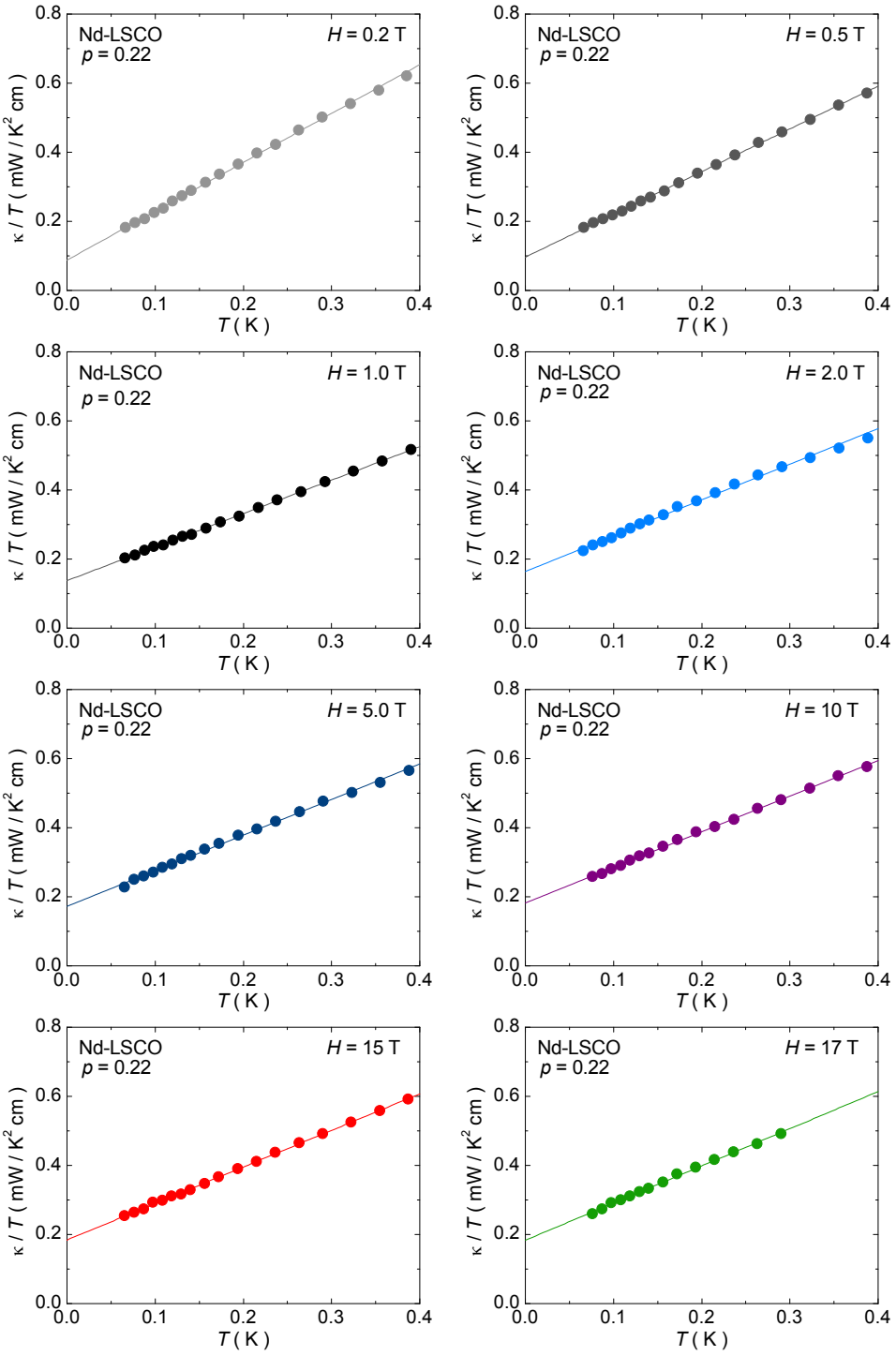

FIG. S3. Thermal conductivity κ versus temperature plotted as κ/T vs T for Nd-LSCO at $p = 0.22$, in magnetic fields as indicated. In all panels the line is a linear fit to the data over the entire range shown.

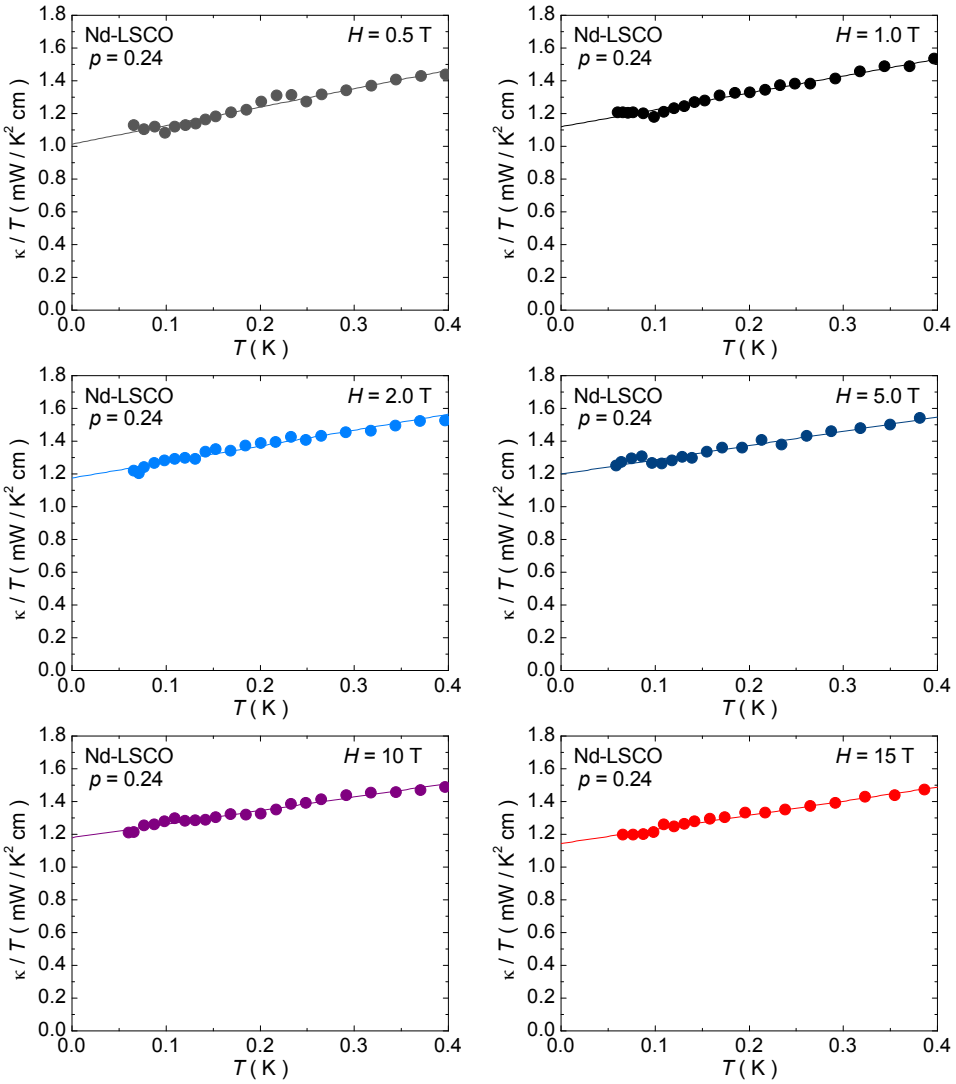

FIG. S4. Thermal conductivity κ versus temperature plotted as κ/T vs T for Nd-LSCO at $p = 0.24$, in magnetic fields as indicated. In all panels the line is a linear fit to the data over the entire range shown.

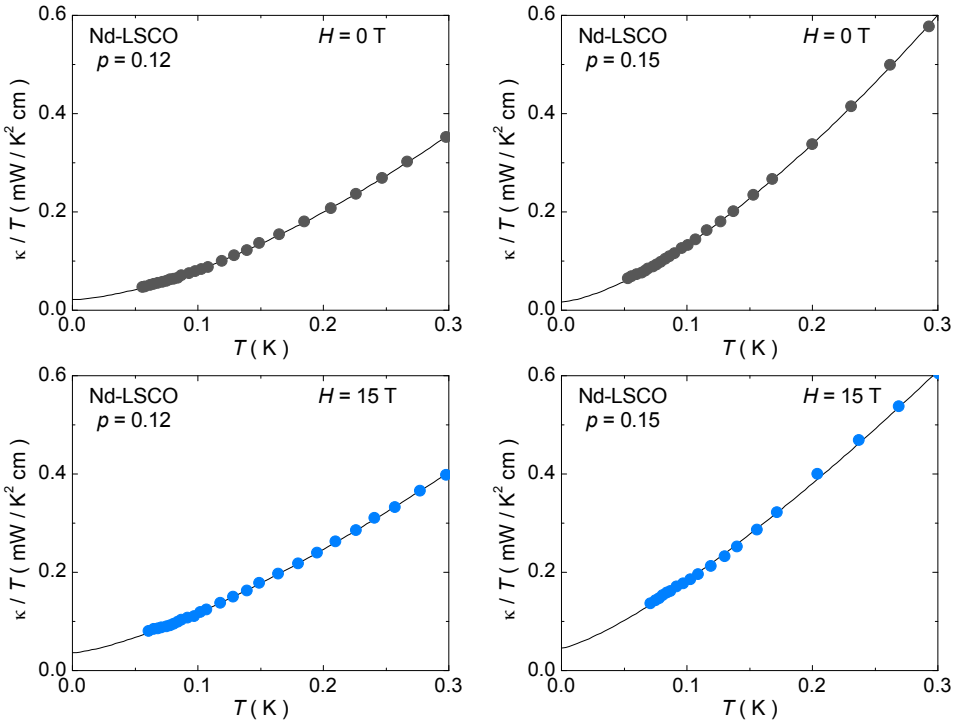

FIG. S5. Thermal conductivity κ versus temperature plotted as κ/T vs T for Nd-LSCO at $p = 0.12$ and 0.15, in magnetic fields as indicated. In all panels the line is a power-law fit of the form $\kappa/T = a + bT^{\alpha}$ to the data over the entire range shown. For $p = 0.12$ the values of α are 1.56 and 1.37 in $H = 0$ and 15 T, respectively. For $p = 0.15$ the values of α are 1.47 and 1.28 in $H = 0$ and 15 T, respectively.

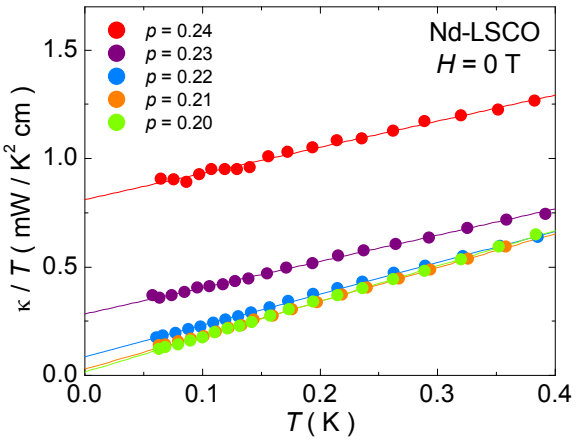

FIG. S6. Thermal conductivity κ versus temperature plotted as κ/T vs T for Nd-LSCO at dopings as indicated, in zero field. The lines are linear fits to the data over the entire range shown

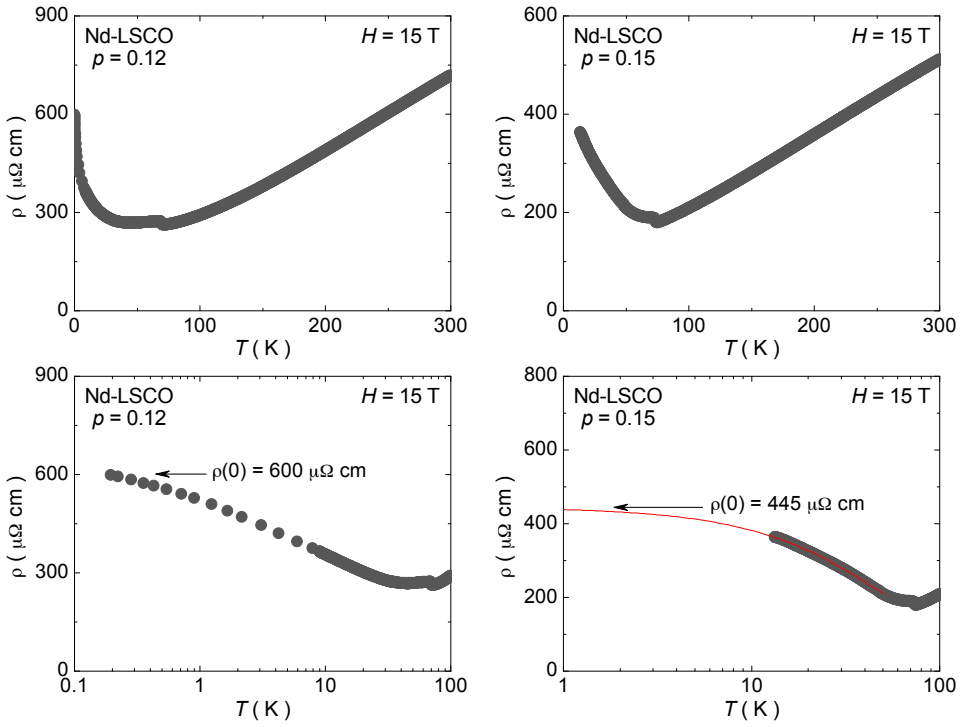

FIG. S7. Electrical resistivity of Nd-LSCO at $p = 0.12$ and 0.15 in $H = 15$ T, shown on a linear scale up to 300 K (top), and on a semi-log scale at low temperature below 100 K.

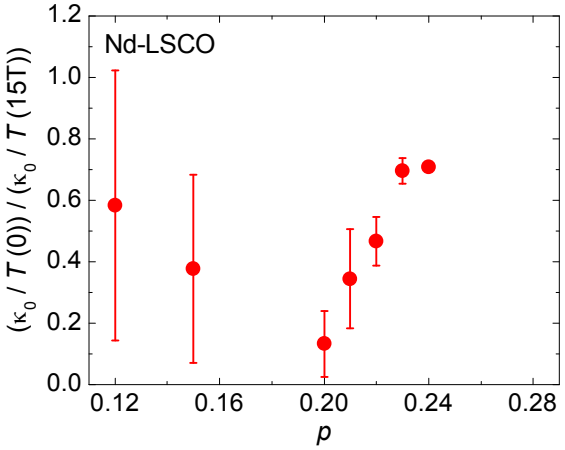

FIG. S8. Ratio of the residual electronic term in the superconducting state at $H = 0$ and in the normal state at 15 T. That this ratio has a minimum at $p = 0.20$ is consistent with the fact that T_c (and presumably the gap maximum Δ_0) is maximal at that doping (Table 1).